

## Advanced flat top laser heating system for high pressure research at GSECARS: application to the melting behavior of germanium

V.B. Prakapenka<sup>a\*</sup>, A. Kubo<sup>a</sup>, A. Kuznetsov<sup>b</sup>, A. Laskin<sup>c</sup>, O. Shkurikhin<sup>d</sup>, P. Dera<sup>a</sup>,  
M.L. Rivers<sup>a</sup> and S.R. Sutton<sup>a</sup>

<sup>a</sup>Consortium for Advanced Radiation Sources, University of Chicago, Chicago, IL 60637, USA; <sup>b</sup>Instituto Nacional de Metrologia, Normalização e Qualidade Industrial – Inmetro, Divisão de Metrologia de Materiais – DIMAT, Xerem, Duque de Caxias, RJ – CEP 25250-020, Brazil; <sup>c</sup>Molecular Technology GmbH, Berlin, 12489, Germany; <sup>d</sup>IPG Photonics Corporation, Oxford, MA 01540, USA

(Received 15 February 2008; final version received 7 March 2008)

Laser heating plays an essential role for *in-situ* high pressure high temperature studies into the physical and chemical properties of materials in the diamond anvil cell (DAC) and minerals at conditions relevant to the Earth's deep interior. High temperature experiments in the multi-Mbar (over 100 GPa) pressure range require the use of very small samples and consequently the utmost stability and controllability of the laser heating is crucial. To accomplish this, we have modified the laser heating system at GSECARS employing newly developed beam shaping optics combined with two diode-pumped, single mode fiber lasers. Varying the settings of the laser heating system, we were able to shape the beam to almost any desired intensity profile and size on the surface of the sample in the DAC, including tight focus, flat top, trident and doughnut types. The advantages and excellent performance of the flat top laser heating (FTLH) technique were demonstrated in melting experiments on germanium in the DAC at pressures up to 40 GPa.

**Keywords:** flat top laser heating; germanium melting; beam shaping; high pressure

### 1. Introduction

Double-sided laser heating combined with synchrotron x-ray radiation for *in-situ* studies in the DAC using diffraction, emission and inelastic scattering methods has been the most productive and widely used high temperature-high pressure technique in past two decades [1–3]. Equations of state, phase transformations, element partitioning, electronic and optical properties of various materials have been successfully studied at conditions relevant to the Earth's interior with the help of lasers [4–7].

High temperature data collected in the DAC are mostly consistent. However, there are some discrepancies in reported results among high pressure research groups performing experiments at different facilities, particularly for determinations of melting temperatures, Clapeyron slopes, elastic constants, and thermal expansion coefficients. Although differences in the samples

---

\*Corresponding author. Email: prakapenka@cars.uchicago.edu

themselves cannot be ruled out, an important contributor to inconsistent results is related to temperature non-uniformity in the analyzed volume.

Because samples used in the DAC are typically 10–50  $\mu\text{m}$  in diameter and 5–20  $\mu\text{m}$  thick at Mbar pressure range, very tightly focused laser and x-ray beams are required, usually 20–40  $\mu\text{m}$  and 5–15  $\mu\text{m}$  in diameter, respectively. The alignment of the laser, x-ray and temperature-measuring optical paths through the diamond anvils is crucial for high quality reproducible data collection. Even with “perfect” alignment, the tightly focused Gaussian or doughnut shaped laser beam as well as instabilities in output power and position of the laser beam on the sample surface result in significant temperature variation within the volume probed by x-rays.

Here we report a new development in on-line, double-sided, laser heating systems based on diode pumped fiber lasers coupled with beam-shaping optics that allows control of the shape of the focused laser beam spot on the sample surface in the DAC with variable diameter from 8 to 40  $\mu\text{m}$ .

## 2. Experimental setup

To maintain the GSECARS (Advanced Photon Source, Argonne National Laboratory, IL) high pressure instrumentation as state-of-the-art research tools and increase the effectiveness of its utilization by a broad high pressure user community, we recently upgraded the double-sided laser heating system located in the 13ID-D station. These modifications were made for improved user-friendliness and system stability and included (1) two new random polarized, diode pumped fiber lasers with an adjustable total power up to 200W at 1.064  $\mu\text{m}$  wavelength, (2) optical components for controlling the shape of the laser beams, (3) relocation of all laser optics on the same lower tier breadboard in order to maximize the mechanical stability of the system, (4) replacement of sample positioning stages with high precision encoded stages, and (5) a few configuration changes in ultra-high temperature measurements for improved accuracy and to free space for the CO<sub>2</sub> laser heating system that is currently being commissioned.

### 2.1. Optical schema

The schematic illustration of the laser heating system is shown in Figure 1. The technical design of the fiber laser allows precise control of the total power in the range from 2 to 200W by changing diode current. For remote laser operation, we are using both RS-232 command code and external analog control options integrated in the EPICS (Experimental Physics and Industrial Control System) database with a user friendly GUI interface. In our previous double-sided laser heating system, two lasers with different beam shapes Gaussian (TEM<sub>00</sub>) and doughnut (TEM<sub>01</sub>) were combined and then split to heat both sides of the DAC [1,8]. Independent power control for both polarized laser beams was achieved using special optics: four motorized wave plates, three polarizing beam splitters and two photodiodes [1,8]. In the new system, we instead use two randomly polarized lasers, one for each side of the DAC with independent power control using an electronic feedback system for the lasers. The electronic power control approach allows improved system stability and simplifies the alignment procedure by removing the sensitive optics used for power alteration of polarized laser beams.

The fiber laser beams, co-axial with a green (532 nm, 1 mW) alignment laser, are guided to the sample position with mirrors (M). Two dichroic mirrors (DM) are used to separate the laser beams and visible radiation coming from the sample for the spectroscopic temperature measurements and sample imaging [1]. X-ray transparent, glassy carbon mirrors (CM) coated with protective

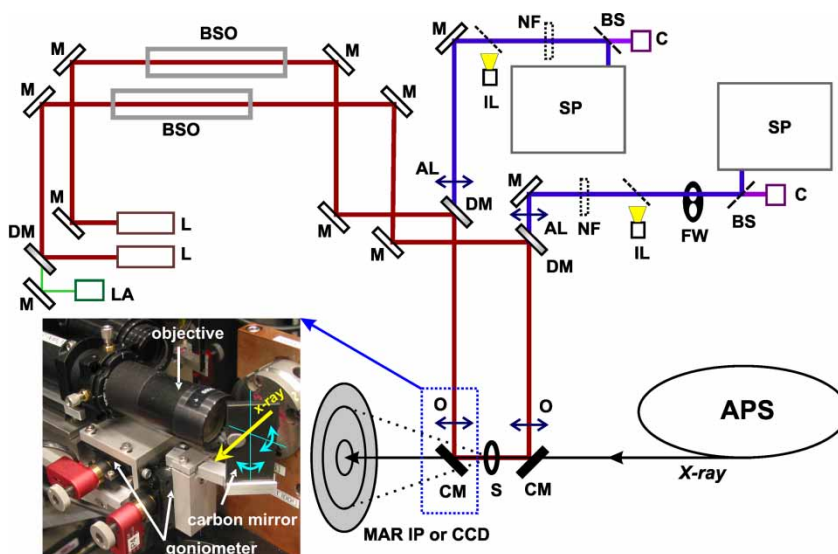


Figure 1. (Color online) Optical schema of the on-line, flat top, double-sided laser heating system at GSECARS, Sector 13, APS. Main components: “L” - two diode pumped single mode CW ytterbium fiber lasers with output power up to 100W each (*IPG Photonics*), “BSO” - beam shaping optics including *FπShaper*® (*MolTech*) and adjustable expander, “M” - dielectric laser mirror, reflectivity is greater than 99% at 1.064 μm (*New Focus*), “CM” - x-ray transparent glassy carbon mirror, 4 mm thick with silver coating reflecting 99.9% in the visible and near IR range, “DM” - laser dichroic mirror, reflecting ~99% of the laser beam at 1.064 μm and transmitting ~90% of visible light (*Optics for Research*), “O” - apochromatic objective lens with 60 mm focal length (*US Laser*), “NF” - notch filter (*Kaiser Optical System*), “SP” - spectrograph (*Holospec f/2.2, Kaiser*), “S” - sample position, “BS” - 45/55 pellicle beamsplitter (*Newport*), “C” - MicroMax CCD camera (*Princeton*), “AL” - achromatic lens with 1000 mm focal length (*Oriel*), “LA” - 1 mW alignment laser (*Lasermate*), “FW” - wheel with neutral filters various optical density (*Thorlabs*), “IL” - fiber illuminator.

silver films are employed for *in-situ* high temperature measurements. Uniquely designed holders with motorized goniometers allow remote tilting of the rectangular (25×50 mm) carbon mirror, with vertex located at the intersection of the x-ray, laser beam and temperature/imaging axes (Figure 1). The main purpose of using this design is to leave the wide open area for detecting x-rays scattered from the sample during laser heating, thereby preserving precise adjustment of optical paths without refocusing of the objective.

The total energy  $E$  emitted at all wavelengths by the blackbody is proportional to the fourth power of the temperature ( $E = \sigma T^4$ , where  $\sigma$  is the Stefan–Boltzmann constant [9]). The consequence of this is a significant increase of signal intensity collected by the CCD detector in the measured wavelength range (600 to 900 nm) as the sample’s temperature increases. Saturation of our CCD detectors with the lowest exposure time (~20 ms) occurs normally at temperatures exceeding ~4000 K (exact saturation temperature depends on sample emissivity). In order to measure ultra high temperatures, we added a wheel with neutral filters (NF) of various optical densities. For correct spectroscopic temperature measurements, the system response is usually calibrated for each filter to be used in the experiment at the beginning of the each run utilizing the procedure described elsewhere [1].

The sample positioning system has recently been upgraded to increase mechanical stability and motion control precision, two improvements that are especially important for sample alignment and positioning during laser heating. One vertical and two horizontal top translation stages are Newport high-precision, high-speed encoded models with resolutions of 60 and 100 nm, respectively.

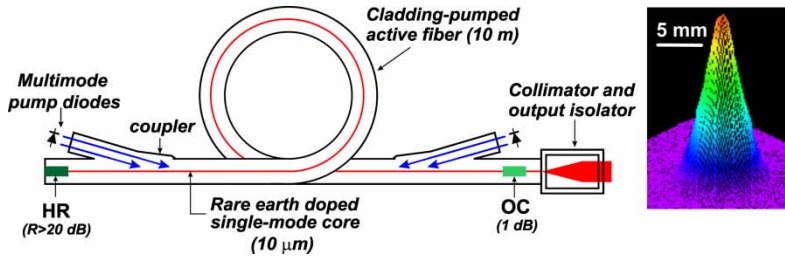


Figure 2. (Color online) Principle schema of the diode pumped fiber laser and 3D intensity profile of output beam measured for the laser installed at GSECARS; “HR” - highly reflective grating and “OC” - output coupler grating.

## 2.2. Diode pumped fiber laser

The new laser heating system at GSECARS employs two diode pumped, single mode CW, ytterbium fiber lasers with output power up to 100 W each. IPG Photonics YLR-SM series fiber laser represents a new generation of diode pumped single mode lasers with a unique combination of high power, ideal beam quality, fiber delivery, high wall-plug efficiency, compactness and reliability.

Schematic illustration of the fiber laser principle is shown in Figure 2. Fiber lasers contain an optical fiber as a laser-active medium with an ytterbium (Yb) doped fiber core enclosed by the pump light cladding into which the light is injected. This laser has an all-fiber design, where all fibers are fusion spliced. It eliminates the need for laser cavity adjustment and alignment. Radiation from the high power, single-stripe, multi-mode pump diodes is absorbed by the core of the Yb-doped active fiber of 10 m length in our configuration. Fiber Bragg gratings written in a single-mode passive fiber are spliced to each end of the active fiber, providing feedback in the laser cavity and forming a classical resonator. The highly reflective (HR) grating at  $1.064\ \mu\text{m}$  has more than 99% reflectivity and the output coupler grating (OC) has about 20% reflectivity. Optical efficiency (Laser output power/Total pump power) is about 75%. Highest beam quality (i.e., closest to the diffraction-limited Gaussian beam shape with a beam propagation factor  $M^2 = 1$ , ISO standard 11146) is attainable when a fundamental mode fiber is used as the optical fiber. The laser-active fiber core in our laser is  $10\ \mu\text{m}$  in diameter where only the fundamental mode  $\text{TEM}_{00}$ , which has an optimal beam quality, can oscillate (Figure 2).

Back reflection from irradiated materials, especially high intensity reflection from samples in the DAC, can cause instability (noise) in the laser operation, decrease the output power and, as a result, degrade the effectiveness, stability and quality of lasing. To protect the laser from back reflection, we are using an output isolator (Figure 2) that is based on rotation of polarization in the magneto-optical Terbium Gallium Garnet (TGG) crystal (Faraday rotator). The isolator is designed to operate at power levels up to 200 W without distortion of the beam quality. Collimated beam diameter at the output of the isolator is 7.5 mm (at an intensity of  $1/e^2$ ) with divergence less than 0.4 mrad.

The high beam quality with nearly ideal Gaussian shape for  $\text{TEM}_{00}$  ( $M^2 < 1.1$ ) mode makes it possible to apply theoretically calculated optical schemes for Gaussian beam shaping at the sample position in the DAC [10]. As a result, a superior stability and laser heating uniformity at extreme conditions can be achieved.

## 2.3. Beam shaping optics

In our laser heating system, the spot size of the focused collimated fiber laser beam with a 60 mm focal length objective was found to be  $\sim 8\ \mu\text{m}$  in diameter (FWHM). Assuming Gaussian shapes

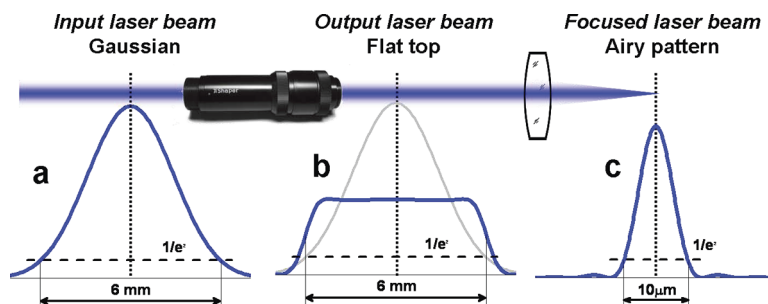


Figure 3. (Color online) Laser beam intensity profiles: a - Gaussian shape 6 mm in diameter at an intensity level of  $1/e^2$ , b - flat top distribution at output of  $\pi$ Shaper®, c - after focusing with 60 mm focal length objective.

for the overlapped x-ray and laser beams, the laser intensity variation within the FWHM of the x-ray beam will be less than 5% when the diameter of the laser beam is at least 5 times larger than that of the 5–10  $\mu\text{m}$  diameter x-ray beam, *i.e.*,  $\sim 25\text{--}50\ \mu\text{m}$ . A simple way to increase the laser beam size on the sample surface is to offset the focal plane from the sample plane. However, in laser heating DAC experiments, the two diamond anvils directly touch the sample on both sides and shifting the DAC relative to the laser focal plane can result in damage to the diamonds by the high power density laser beam. Therefore we have instead introduced beam shaping optics based on the  $\pi$ Shaper® device that allows us not only to control the beam size in the focal plane but also its shape.

The concept of  $\pi$ Shaper®'s operation is illustrated in Figure 3. The Gaussian intensity distribution of a collimated TEM<sub>00</sub> laser beam (Figure 3a) can be converted with  $\pi$ Shaper® to a flat top distribution as shown in Figure 3b (similar to the Greek letter  $\Pi$ ). The technology of energy conversion makes it possible to create almost arbitrary intensity distribution of output beams [10]. In the case of flat top distribution,  $\pi$ Shaper® is a telescope, related to the so called refractive field mapping systems, where the intensity profile is transformed by applying special optical surfaces in a controlled manner. One of the basic features is zero wave aberration for the entire system [10]. These features distinguish the  $\pi$ Shaper® from integration type homogenizers where uniform intensity is provided by applying multi-lens optical components and mixing parts of the original beam (beamlets) in a certain working plane. In contrast to beam integrators, the flat top intensity profile created by  $\pi$ Shaper® stays invariable over a long distance (typically several hundreds of mm) thereby simplifying its application in real systems. As distinct from other field mapping beam shaping systems [11,12], the  $\pi$ Shaper® has some important additional advantages. The Galilean telescope design guarantees the beam shape transformation without internal focusing, which is important for high-power and short-pulse applications. With optimized anti-reflection coatings, it is possible to reach nearly 99% transmission of laser radiation preventing heat-induced instability of the optical system, a great advantage over the diffraction type homogenizers.

Due to the strict requirement for the size of the Gaussian beam at  $\pi$ Shaper®'s input, we use an adjustable de-expander with magnification of 0.8 to convert our laser beam spot size from 7.5 mm to 6 mm in diameter at  $1/e^2$ . A flat top laser beam of  $\sim 6$  mm in diameter at the output of the  $\pi$ Shaper® was readily produced. It is well known that in terms of mathematical description, the intensity distribution in the focal plane of the lens is a result of a Fourier transformation of the incident intensity distribution. Hence the flat top intensity distribution formed by  $\pi$ Shaper® will be converted to an Airy type pattern at the focal plane of our objective (Figure 3c). Detailed theoretical calculations predict the possibility to shape the laser beam to trident and doughnut type intensity distributions in the focal plane by changing the internal settings of the expander and the  $\pi$ Shaper® used in our system, however, we were unable to produce such shapes in the

range of sizes suitable for laser heating in the DAC. Note that we are using the same objective for sample imaging, laser focusing and temperature measurements, therefore the objective-sample distance in our system is fixed [1].

Fascinating options for beam profile modification appeared, however, when we reversed the orientation of the  $\pi$  Shaper®, i.e. with the Gaussian laser beam entering the nominal  $\pi$  Shaper® output port. In this case, the Gaussian beam converts to a beam with most energy concentrated in the central part. At the distance of  $\sim 1200$  mm (objective- $\pi$  Shaper® distance in our experiments), the beam profile has an intensity distribution approximating a so called super-Gaussian function (Figure 4, [10]). Since the wavefront of a beam focused by a lens has a strong and variable curvature in space around the focal point, the beam intensity profiles in the focal plane and nearest planes are also variable. A few examples of calculated intensity distributions and corresponding real images of the laser heated spot on Pt foil ( $25\ \mu\text{m}$  thickness) are presented in Figure 5. Varying the settings of the  $\pi$  Shaper® and the de-expander, we were able to shape the beam on the sample surface to almost any desirable intensity profile and size including tight focus, flat top, trident and doughnut types, while sample and objective positions were fixed.

Although, the optical system described above offers flexibility for beam shaping, the operation and control are non-trivial and require some experience. Therefore a new user-friendly optical

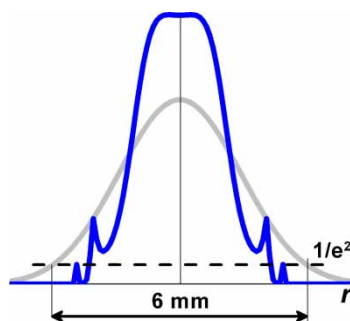


Figure 4. (Color online) Theoretically predicted super-Gaussian intensity profile of laser beam, converted by reverse oriented  $\pi$  Shaper®, at input of objective positioned at 1200 mm from  $\pi$  Shaper®.

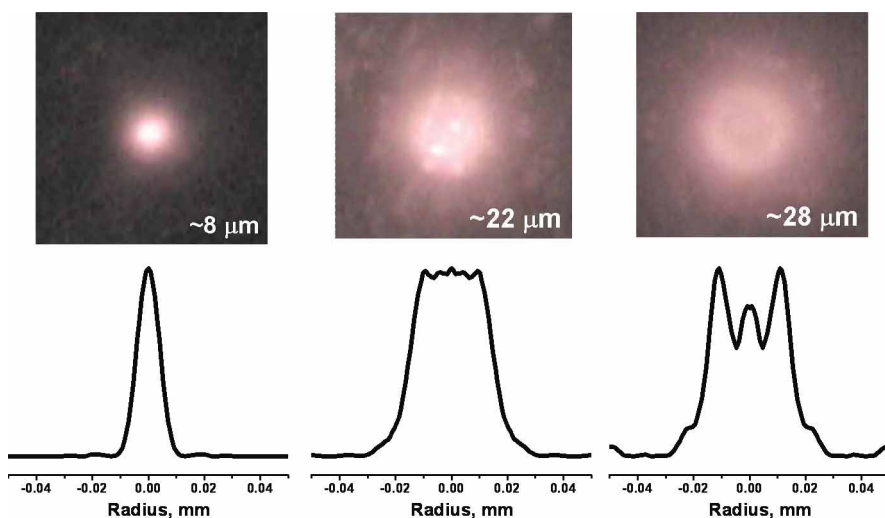


Figure 5. (Color online) Typical examples of experimentally observed images of laser heating spots on a Pt foil ( $25\ \mu\text{m}$  thickness) and corresponding theoretically predicted intensity profiles of focused super-Gaussian beam at different settings of  $\pi$  Shaper® and expander: a – tight focus, b – flat top, c – trident type.

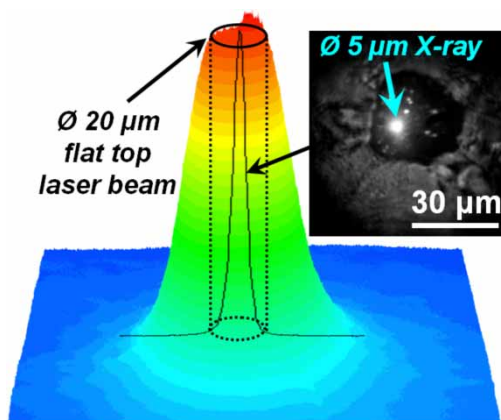


Figure 6. (Color online) Experimentally measured 3D shape of flat top laser heating spot (25  $\mu\text{m}$  in diameter, FWHM) formed with *F $\pi$ Shaper*® on the surface of Pt foil in the DAC at 10 GPa and  $\sim 1500$  K and intensity profile of x-ray (5  $\mu\text{m}$  in diameter, FWHM) induced luminescence from NaCl pressure medium with corresponded image shown in insert.

component has been developed for direct conversion of a Gaussian laser beam into a beam with an intensity profile similar to an Airy distribution, that after focusing results in a flat top shaped beam on the sample surface. This beam shaping system, *Focal  $\pi$ Shaper*® (*F $\pi$ Shaper*®), is implemented as a unit capable of operating with laser beams of various sizes ranging from 5 to 8 mm in diameter and has been shown to be less sensitive to misalignments. Similar to the  *$\pi$ Shaper*®, varying the settings of the *F $\pi$ Shaper*® and adjustable expander makes it possible to shape the beam to almost any desirable intensity profile and size on the sample surface.

For example, Figure 6 shows the overlap of an experimentally measured 3D shape of the flat top laser heating spot (25  $\mu\text{m}$  in diameter, FWHM) formed with *F $\pi$ Shaper*® on the surface of Pt foil in the DAC at 10 GPa and  $\sim 1500$  K with the cross-section intensity profile of x-ray (5  $\mu\text{m}$  in diameter, FWHM) induced luminescence from the NaCl pressure medium. It is clear that the entire x-ray beam lies within the uniformly heated sample. Since total thermal radiation of the sample, measured with a CCD camera, is proportional to the fourth power of the temperature, the slight variation of intensity within the flat top will not significantly affect temperature distribution. Averaging a number of experimental data, we have found that the standard deviation of mean temperature within the flat top for our system is less than 1%.

Thus with the modifications of the optical system described above, one can expect that the application of a flat top double-sided laser heating system for *in-situ* high-pressure high-temperature studies in the DAC with x-ray synchrotron radiation will significantly reduce temperature gradients within the x-ray probe volume.

### 3. Results and discussion

One of the most challenging experiments related to the laser heating technique in the DAC is an unambiguous x-ray based detection of melting by recording diffuse x-ray scattering from molten materials [13–16]. So far, only at GSECARS has it been possible to measure high quality x-ray scattering spectra from laser-melted materials at high pressures suitable for structure analysis [14]. Moreover, we have shown recently that by changing the cooling speed (quench rate) of molten samples at high-pressures, it is possible to control sample grain size and to synthesize nanocrystalline or microcrystalline materials *in-situ* at extreme conditions [15].



In DAC experiments on melting, the experimental configuration of the laser heating and sample preparation method may affect the characteristics of the melting process. Such differences are likely to be major sources of disagreements between the results of various studies. An example of such discrepancies is illustrated by a recent experiment on the melting of lead carried out at ESRF (beamline ID-27) involving the detection of a diffuse x-ray scattering ring or using second-scale time resolved x-ray diffraction based on appearance-disappearance of lead single crystal spots [16]. The authors claim major improvement over previous optical and x-ray detection based techniques by reducing the scattering collection time to  $\sim 2$  s, citing that the typical melting phenomena lifetime in the DAC can be as low as 1 s. This conclusion about the short lifetime of molten sample in a DAC disagrees, however, with the results reported earlier where typical x-ray scattering collection time from molten materials in laser heated DAC was at least  $\sim 10$  s up to pressures  $\sim 65$  GPa [14,15]. The main reason for this inconsistency could lie in the specifics of the sample preparation and laser heating technique configuration used for these studies. It is well known that Gaussian laser power distribution in a heating spot tends to excavate the sample at temperatures close to the melting point due to solid state diffusion enhanced by huge temperature and pressure gradients. In order to successfully reach the melting temperature and maintain the molten sample for a sufficient time for x-ray measurements, the sample should be spherical in shape with a size commensurate with that of the laser beam. This requirement is very challenging to fulfill in laser heated DAC experiments and requires not only a specific sample preparation procedure, but also a well-defined pressure temperature history. The equal thickness of insulating layers in a DAC is also important for such melting experiments. The newly developed laser heating setup at GSECARS based on two fiber lasers and beam shaping optics forming a flat top heating spot on sample surface in the DAC allowed us to more closely approximate the ideal laser heating geometry and to overcome other complications associated with the laser heating in the DAC. Here we demonstrate the application of flat top laser heating (FTLH) in the DAC for x-ray based melting detection for germanium up to pressures of  $\sim 40$  GPa using standard loading techniques for preparation of the sample.

At ambient pressure germanium has the diamond-type structure with space group  $Fd\bar{3}m$  (Ge-I) and is characterized by a relatively low melting temperature,  $\sim 1211$  K. With increasing pressure, germanium undergoes a semiconductor-to-metal transition to the high-pressure tetragonal phase with space group  $14_1/amd$  (Ge-II) [17]. This transition is very sluggish and takes place over a broad pressure range of 7–12 GPa at room temperature. The melting temperature decreases to  $\sim 833$  K at  $\sim 8.7$  GPa where a Ge-I:Ge-II:liquid triple point has been reported [18]. The maximum pressure at which the experimental melting point has been reported is  $\sim 11$  GPa.

Single crystal germanium polished down to a thickness of  $20\ \mu\text{m}$  was loaded in a symmetric type DAC with  $300\ \mu\text{m}$  culet anvils. A rhenium gasket of  $250\ \mu\text{m}$  initial thickness was indented to the thickness of  $30\ \mu\text{m}$ . The sample was sandwiched between two polycrystalline MgO wafers of  $5\ \mu\text{m}$  thickness that served as thermal insulation layers and a pressure standard. The MgO was dried at 1300 K for 1 day to eliminate moisture. The DAC was sealed in an argon atmosphere. Double sided FTLH combined with on-line high resolution angle-dispersive x-ray diffraction was used at GSECARS (Sector13, APS). The laser beam was focused to  $25\ \mu\text{m}$  in diameter (FWHM) at the sample surface with a flat top of  $\sim 20\ \mu\text{m}$  in diameter. The scattered x-ray radiation (beam size  $\sim 5 \times 5\ \mu\text{m}$  at 40 keV) was collected with a MAR-CCD detector for 5–60 s. The temperature was calculated by fitting the slope of the thermal emission spectra to a grey-body Plank radiation function [1]. Special care was taken for precise alignment of x-ray and laser beams with temperature measurement paths. We used visual observation of x-ray induced luminescence from the sample (mainly from MgO) with high sensitivity CCD cameras from both sides of the DAC to align the optical paths with a reference mark on the monitor screens [14,15].

Two diffraction patterns collected from Ge during laser heating (1150 and 1280 K) at 19 GPa are shown in Figure 7 with corresponding spectra integrated using the Fit2d program [19] in Figure 8.



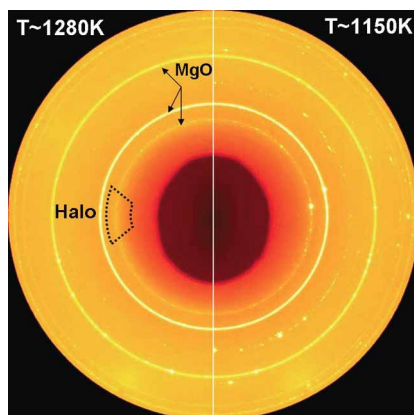


Figure 7. (Color online) 2D images collected with the MAR CCD detector for 60 s from molten and partially crystalline Ge at 19 GPa and temperatures of  $\sim 1280$  K (a) and  $\sim 1150$  K (b), respectively. Sharp continuous lines are from MgO pressure medium.

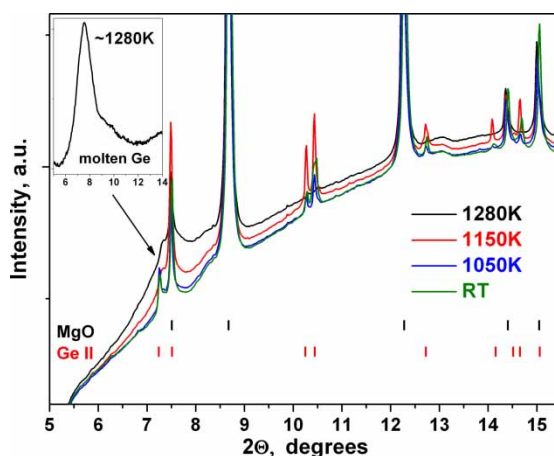


Figure 8. (Color online) Selected diffraction spectra of Ge in MgO pressure medium collected for 60 s at  $\sim 19$  GPa and different temperatures, from top to bottom: 1280 K, 1150 K, 1050 K and room temperature. The calculated peak positions for MgO (top) and Ge II (bottom) solid phases are shown by the tick marks. Typical background subtracted diffuse scattering from liquid Ge is shown in insert.

The sharp lines in the spectrum at 1280 K are from the polycrystalline MgO pressure medium while the diffuse halo is from the liquid phase of completely molten Ge. Insert on Figure 8 shows pure diffuse x-ray scattering from laser molten liquid Ge at  $\sim 1280$  K obtained using high temperature crystalline diffraction pattern collected at  $\sim 1050$  K as a background. The x-ray detector exposure time was 60 s indicating that the lifetime of laser melted materials in the DAC is certainly not limited to 1 s, as it was suggested in recent studies [16]. As one can see, the liquid state of Ge can be kept for at least an order of magnitude longer time when the flat top laser heating system is used. Decreasing the temperature to 1150 K causes the Ge to partially recrystallize. The temperature distribution along the laser beam depends sensitively on sample thickness and laser beam size relation [20]. It is obvious that in our configuration, when the sample thickness of  $\sim 20$   $\mu\text{m}$  is comparable with size of the laser beam ( $\sim 25$   $\mu\text{m}$ ) at temperatures close to the melting point, coexistence of both liquid and solid phases can be observed. Only the solid phase of Ge-II was detected at 1050 K. As a consequence, the melting temperature of Ge at 19 GPa lies between

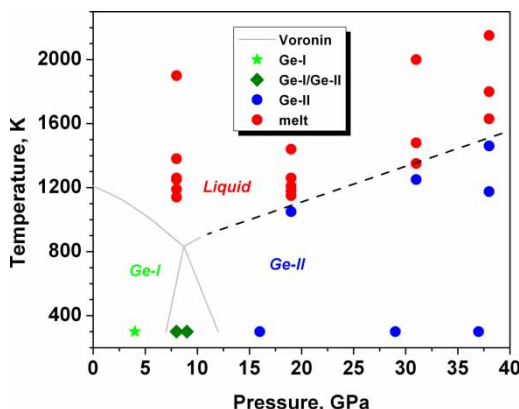


Figure 9. (Color online) P-T phase diagram of Ge. Continuous lines – Voronin et al. [18], scattered symbols – experimental points from this study, and dashed line - melting curve of Ge II defined in this study.

1050 K and 1150 K and hence we infer a melting temperature of 1100 K with  $\pm 50$  degrees uncertainty. The remaining data points presented in Figure 9 were treated in a similar manner. The details of high pressure and high temperature induced solid state phase transformations of germanium will be reported elsewhere.

The P-T phase diagram of germanium based on the results of our data analysis is shown in Figure 9. Our data on melting temperatures are in good agreement with previous *in-situ* studies using a large volume press with the energy dispersive x-ray diffraction technique [18]. The melting curve for the Ge-II phase determined in this study is consistent with the triple point of Ge-I:Ge-II:liquid defined in early studies within experimental uncertainty [18,21]. This experiment with Ge clearly demonstrates that high accuracy data collected with the newly developed advanced FTLH DAC technique in combination with synchrotron based methods can be successful for determination of phase diagrams in a wide high P-T range. Moreover, the capability to maintain the molten sample in the DAC for a relatively long time (at least 60 s) allows one to collect high quality x-ray scattering data at 3<sup>rd</sup> generation synchrotrons even from low-Z molten materials, and can be used to accomplish the most challenging experiments at extreme conditions associated with melting. As a result, the very demanding DAC experiments at multi-Mbar pressures can now be routinely conducted at GSECARS *in-situ* at ultra high temperatures by means of the on-line, double-sided, flat top laser heating system in combination with synchrotron x-ray techniques.

#### 4. Summary

We have described a new, advanced laser heating technique based on the use of diode pumped fiber lasers with beam shaping optics, allowing the formation of flat top laser heating spots on the surface of samples in the DAC. Uniform radial temperature distribution within the heating spot is very important for all high temperature-high pressure studies in the DAC, especially for the on-line combination of laser heating with high resolution x-ray synchrotron techniques including diffraction, emission, elastic and inelastic scattering. The new optical device *F $\pi$ Shaper*® was built based on the results of a number of laser heated experiments conducted at GSECARS, in collaboration with MolTech GmbH. It is simple to use and the relatively straightforward alignment of beam shaping optics allows *F $\pi$ Shaper*® to be integrated into almost any laser heating system.

The example of the very challenging high pressure melting of Ge demonstrates the significant advantages of using the flat top laser heating technique compared to the typical laser heating

and time-resolved setups. During FT laser heating the molten sample does not escape from the homogeneously heated area, as is usually observed for Gaussian or doughnut type laser spots in the DAC. The FTLH method opens a new era in high temperature-high pressure studies using diamond anvil cell with combination of advanced synchrotron as well as lab techniques, and will lead to superior quality high temperature measurements including equation of state, melting curve, phase transformation, element portioning, elastic, electronic and optical properties.

## Acknowledgements

The authors thank G. Shen for the initial development of the laser heating system at GSECARS, N. Lazarz, F. Sopron and C. Pullins for technical support, D. Shim for help with data collection and S. Urakawa for discussion. This work was performed at GeoSoilEnviroCARS (Sector 13), Advanced Photon Source (APS), and Argonne National Laboratory. GeoSoilEnviroCARS is supported by the National Science Foundation - Earth Sciences (EAR-0622171) and Department of Energy - Geosciences (DE-FG02-94ER14466). Use of the Advanced Photon Source was supported by the U.S. Department of Energy, Office of Science, Office of Basic Energy Sciences, under Contract No. DE-AC02-06CH11357.

## References

- [1] G. Shen, M. Rivers, Y. Wang et al., *Rev. Sci. Instrum.* 72 (2001), p. 1273
- [2] E. Schultz, M. Mezouar, W. Crichton et al., *High Pressure Research* 25 (2005), p. 71.
- [3] T. Watanuki, O. Shimomura, T. Yagi et al., *Rev. Sci. Instrum.* 72 (2001), p. 1289.
- [4] T.S. Duffy, *Rep. Prog. Phys.* 68 (2005), p. 1811–1859.
- [5] L. Dubrovinsky, N. Dubrovinskaia, O. Narygina et al., *Science* 316 (2007), p. 1880.
- [6] J.-F. Lin, G. Vankó, S.D. Jacobsen et al., *Science* 317 (2007), p. 1741.
- [7] K. Hirose, *Rev. Geophys.* 44 (2006), p. 1.
- [8] G. Shen, V.B. Prakapenka, P.J. Eng et al., *J. Synchrotron Rad.* 12 (2005), p. 642.
- [9] G. Rybicki and A.P. Lightman, *Radiative Processes in Astrophysics*, Wiley-Interscience, New York, 1979.
- [10] F.M. Dickey and S.C. Holswade, *Laser Beam Shaping: Theory and Techniques*, Marcel Dekker, Inc., New York, 2000.
- [11] S. Bollanti, P.D. Lazzaro, and D. Murra, *Eur. Phys. J. Appl. Phys.* 28 (2004), p. 179.
- [12] J.J. Yang and M.R. Wang, *Opt. Eng.* 42 (2003), p. 3106.
- [13] D. Errandonea, M. Somayazulu, D. Hausermann et al., *Journal of Physics: Condensed Matter* 15 (2003), p. 7635.
- [14] G. Shen, V.B. Prakapenka, M.L. Rivers et al., *Phys. Rev. Lett* 92 (2004), p. 185701.
- [15] V.B. Prakapenka, G. Shen, M.L. Rivers et al., *J. Synchrotron Rad.* 12 (2005), p. 560.
- [16] A. Dewaele, M. Mezouar, N. Guignot et al., *Phys. Rev. B* 76 (2007), p. 144106.
- [17] A. Mujica, A. Rubio, A. Muñoz et al., *Rev. Mod. Phys.* 75 (2003), p. 863.
- [18] G.A. Voronin, C. Pantea, T.W. Zerda et al., *J. Phys. Chem. Solids* 64 (2003), p. 2113.
- [19] A.P. Hammersley, S.O. Svensson, M. Hanfland et al., *High Pressure Research* 14 (1996), p. 235.
- [20] B. Kiefer and T.S. Duffy, *J. Appl. Phys.* 97 (2005), p. 114902.
- [21] V.V. Brazhkin, A.G. Lyapin, S.V. Popova et al., *Phys. Rev. B* 51 (1995), p. 7549.